

SIMULTANEOUS GAIN AND BANDWIDTHS ENHANCEMENT OF A SINGLE-FEED CIRCULARLY POLARIZED MICROSTRIP PATCH ANTENNA USING A METAMATERIAL REFLECTIVE SURFACE

S. Chaimool

Wireless Communication Research Group
Department of Electrical Engineering, Faculty of Engineering
King Mongkut's University of Technology North Bangkok
Bangkok, Thailand

K. L. Chung

Department of Electronic and Information
Hong Kong Polytechnic University
Hong Kong, China

P. Akkaraekthalin

Wireless Communication Research Group
Department of Electrical Engineering, Faculty of Engineering
King Mongkut's University of Technology North Bangkok
Bangkok, Thailand

Abstract—This paper proposes a metamaterial reflective surface (MRS) as a superstrate for a single-feed circularly polarized microstrip patch antenna (SFCP-MPA). It illustrates a simultaneous enhancement on antenna gain, impedance bandwidth (ZBW) and axial-ratio bandwidth (ARBW) by adding the MRS atop the SFCP-MPA. The MRS can enhance the ZBW and ARBW by 3.5 and 9.9 times, respectively, compared to the circularly polarized patch source. Moreover, the gain of the CP-MPA with the MRS is 7 dB higher than that of the conventional CP-MPA. The small spacing between the MRS and patch source is another merit in the present design, which is as low as $\lambda_0/16$, as it results in a low-profile antenna design that well suits modern wireless communications.

Corresponding author: S. Chaimool (sarawuth@kmutnb.ac.th).

1. INTRODUCTION

Circularly polarized (CP) antennas can reduce the loss caused by the misalignment between transmitting and receiving antennas. CP wave in the broadside direction is generated when two orthogonal modes are excited with equal amplitude with quadrature phases. Currently, circularly polarized microstrip patch antennas (CP-MPAs) are widely used, particularly in satellite and wireless communications, since they are compact, lightweight and cost-effective. Circular polarization can be achieved by using a microstrip patch antenna (MPA) with a single-feed [1]. Two nearly degenerated resonant modes in single-feed MPAs are usually achieved by cutting diagonal slits or attaching stubs to the corners of a square patch. When using these approaches, however, the impedance bandwidth (ZBW) and 3-dB axial-ratio bandwidth (ARBW) are narrow because of the high unloaded Q -factor of MPAs. Therefore, various designs have been proposed in extant literature to improve their ZBW and ARBW, including the use of dual-feed patch [2] and sequential rotation array [3]. As an alternative to increase both impedance bandwidth and gain, the CP stacked electromagnetically coupled patch antenna was proposed by Chung et al. [4]. However, for good CP performance such configurations require the use of a wideband power divider. A feeding network such as a Wilkinson power divider or a quadrature hybrid may cause additional conductor and dielectric losses, not to mention the already complicated antenna structure. Several techniques have been used to enhance the antenna gain of linearly polarized microstrip patch antennas (LP-MPAs). Use of the electromagnetic band-gap (EBG) and frequency selective surface (FSS) as a superstrate has been proposed by Pirhadi et al. [5]. Also, use of metamaterials as antenna substrates has been proposed by Enoch et al. [6] and Wu et al. [7]. An interesting class of metamaterials (MTMs), known as the zero-index medium, exhibits a remarkable influence on wave propagation properties. As refractive index $n = \sqrt{\epsilon\mu}$, the structured zero-index medium can be realized by making its effective permittivity and/or effective permeability approach zero at the frequency of interest. Enoch et al. [6] demonstrated that radiation beam of a source embedded in MTM will be refracted in a direction very close to the normal when the refractive index (n) is close to zero, in some frequency bands. Furthermore, *epsilon*-near-zero (ENZ) or *mu*-near-zero (MNZ) may show other interesting features such as the efficiency enhancement of a waveguide [8], and the transparent media and transmission enhancements [9]. Gupta was the pioneer in the creation of highly directive radiation beam antennas using permittivity less than unity [10]. The metallic grid is made of the simplest type of

MTMs used to form ENZ medium; many researchers have used this property to design high directive antennas [6, 7, 11]. It is indicated that if planar MNZ- or ENZ-MTMs is used as a superstrate for an antenna, the radiation beam would be confined resulting in gain being enhanced. In addition, the metamaterial reflective surface (MRS) can enhance both the impedance bandwidth and gain, simultaneously, of a low-cost LP-MPA [12]. According to our literature review, most papers focus on the superstrate's effects in linearly polarized antennas. Only a few have reported simultaneous gain and bandwidths enhancement for the CP-MPAs [13–15]. In [13, 14], the use of FSS superstrates to enhance directivity was proposed, but only gain enhancement has been achieved; neither ARBW nor ZBW improved. In [15], a CP-MPA was integrated with the planar periodic EBG structure to improve both the ZBW and ARBW, to the extent possible, but gain enhancement was not significant. Therefore, simultaneous enhancement of ZBW, ARBW, antenna directivity and gain bandwidth for CP-MPA has long been a challenging task. This has motivated us to study a new method that uses MRS as a superstrate for CP-MPA.

This paper proposes a novel metamaterial reflective surface (MRS) as a superstrate for a single-feed circularly polarized microstrip patch antenna at 2.45 GHz. The design objective here is to obtain simultaneous enhancement for antenna gain, impedance bandwidth, axial-ratio bandwidth and gain bandwidth. The proposed CP antenna has a simple, low profile, and yet a low-cost structure. The planar MRS is composed of 4×4 square rings joined with diagonal-strips (SQR-DS). The MRS exhibits the unusual properties of a *mu*-near-zero (MNZ) and a high-epsilon (high- ϵ) parameter when illuminated by a normal incident CP wave.

2. ANTENNA DESIGN AND THE MRS PERFORMANCE

2.1. Antenna Design

The configuration of the proposed antenna is shown in Fig. 1. It consists of an array of 4×4 square rings with 135° diagonal-strips (SQR-DS) suspended over a conventional CP patch source at a distance of h . The driven patch is perturbed from a square patch of $30 \times 30 \text{ mm}^2$ by cutting two opposite corners with a truncation depth of b . The truncated patch is printed on an inexpensive FR-4 substrate with a dielectric constant (ϵ_{r1}) of 4.2 and a thickness (h_1) of 1.6 mm. A SMA connector is used as a coaxial feed and is placed on the y -axis at a distance of f_p from the center of the source patch. The truncated square patch has a length (L) of 30 mm and $b = 7$ mm, which stimulates

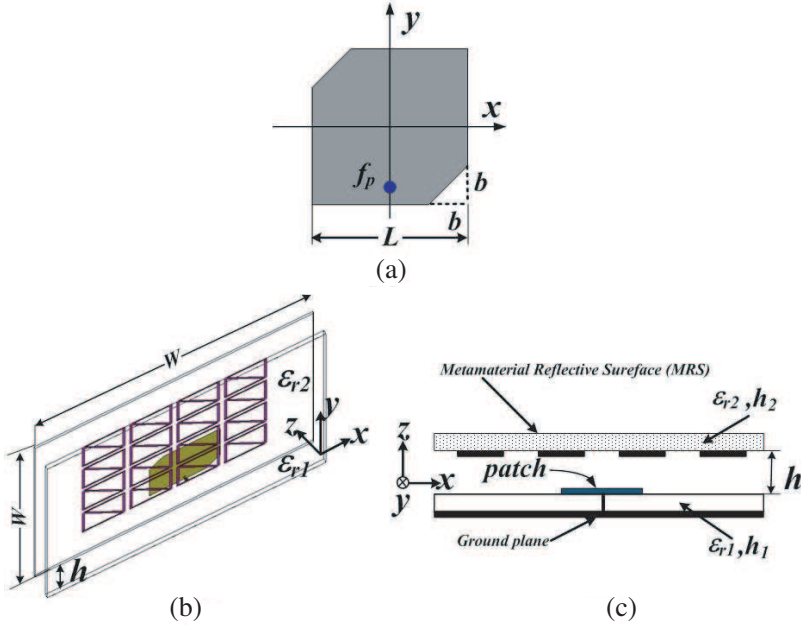


Figure 1. (a) Dimension of the truncated microstrip patch. (b) Configuration of the truncated microstrip patch antenna under the 4×4 single square rings with diagonal-strips (SQR-DS) and (c) the cross sectional view.

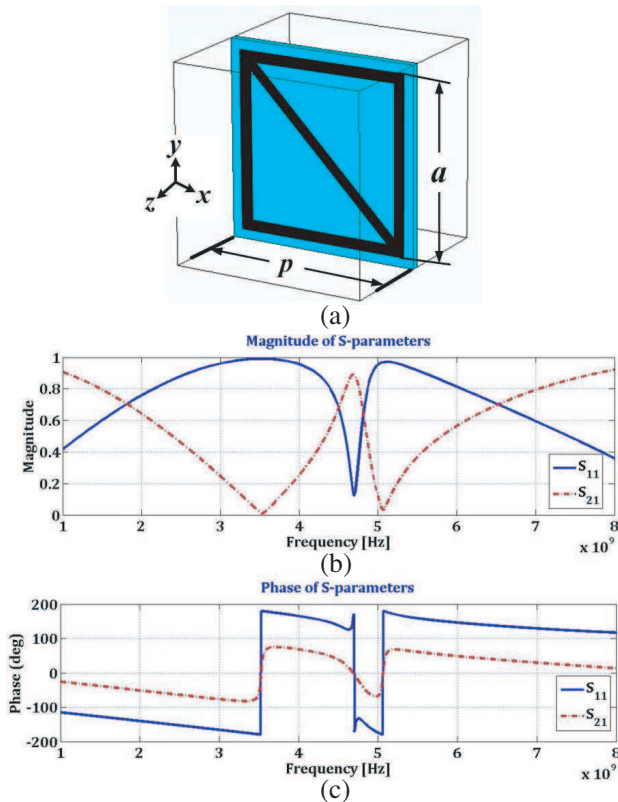
the source antenna to radiate a left-hand CP wave at 2.45 GHz. The square ground plane has the same dimensions as the MRS, lengths (W) of whose four sides are all 200 mm.

2.2. The MRS Performance

Since the MRS under design is a periodic structure, we compute the scattering parameters (S -parameters) by modeling a single unit-cell with a periodic boundary condition using the CST Microwave Studio. This paper proposes the use of the SQR-DS to realize a high gain while enhancing bandwidths of impedance, gain and AR. In the geometry shown in Fig. 2(a), we set the size of the square unit-cell to $p = 20$ mm and $a = 18$ mm. The width of the copper strip is 1 mm. The MRS structure is formed by using a FR-4 dielectric slab with a thickness of $h_2 = 0.8$ mm and a dielectric constant $\epsilon_{r2} = 4.2$. There are several methods for extraction of effective constitutive parameters for MTM structures. The most popular approach is extraction from transmission

and reflection characteristics of a MTM. The complex normalized wave impedance (z) and refractive index (n) are retrieved from the S -parameters, and then effective permittivity (ϵ_{eff}) and permeability (μ_{eff}) are computed from n and z values [16].

Here, the incident electromagnetic wave is polarized with the magnetic field parallel to the SQR-DS resonator plane ($\mathbf{H} \parallel y$), while the electric field polarizes along the x -axis ($\mathbf{E} \parallel x$). Consequently, the propagation direction of wave vector \mathbf{k} is along the z -axis (normal-incidence). The magnitudes and phases of the S -parameters (S_{11} and S_{21}) are shown in Fig. 2(b) and Fig. 2(c), respectively. The normalized wave impedance and refractive index are shown in Fig. 2(d) and Fig. 2(e), respectively. It is worth noting that the MRS does not belong to a double negative medium (DNG) in frequency ranges of 3.5 GHz to 4.5 GHz and 5.2 GHz to 7.0 GHz, though the negative real parts of the refractive index (n') are obtained. The reason is $n' = \epsilon'z' - \epsilon''z''$, so it is possible to have $n' < 0$, provided that $\epsilon''z'' > \epsilon'z'$. Effective



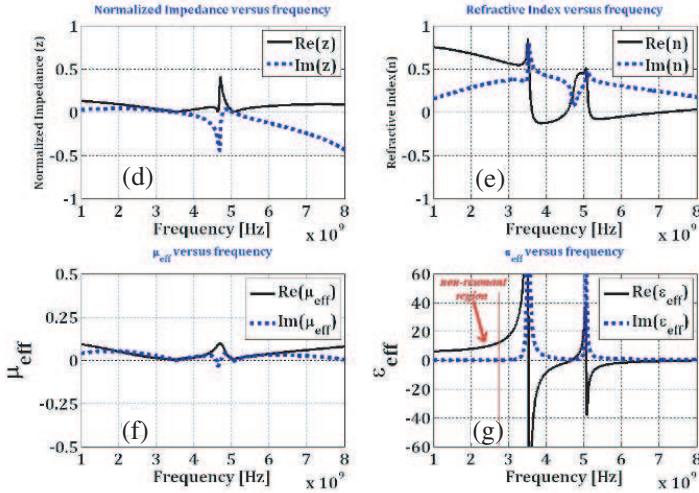


Figure 2. (a) Dimension of the unit cell, simulated S_{11} and S_{21} . (b) Magnitudes and (c) phases of the single square ring with a diagonal-strip (SQR-DS) unit cell at the normal-to- xy plane incidence, the retrieved effective constitutive parameters of the SQR-DS. (d) Normalized wave impedance (z). (e) Refractive index (n). (f) Effective permeability (μ_{eff}) and (g) Effective permittivity (ϵ_{eff}).

permeability and permittivity are extracted and shown in Fig. 2(f) and Fig. 2(g), respectively. These figures confirm the obtained MNZ and high- ϵ lying between 2.0 and 3.2 GHz. In Fig. 2(g), it is observed that resonances occur near 3.5 GHz and 5.0 GHz, frequencies at which the effective permittivity (ϵ_{eff}) exhibits the Lorentzian line shape.

3. SIMULATED AND MEASURED RESULTS

IE3D and the CST electromagnetic simulators were used to simulate the antenna performance and compute MRS properties, respectively. Antenna performances were measured by an Agilent vector network analyzer E8363C and the SATIMO near-field anechoic chamber at the Chinese University of Hong Kong. Impedance bandwidth (ZBW) is defined as a range of frequencies over which the input return-loss is not smaller than a designed value, of 10 dB, whereas the axial-ratio bandwidth (ARBW) is defined as a range of frequencies over which the axial-ratio does not exceed a designed value, 3 dB in this study. The performance of the conventional truncated-corner CP patch antenna

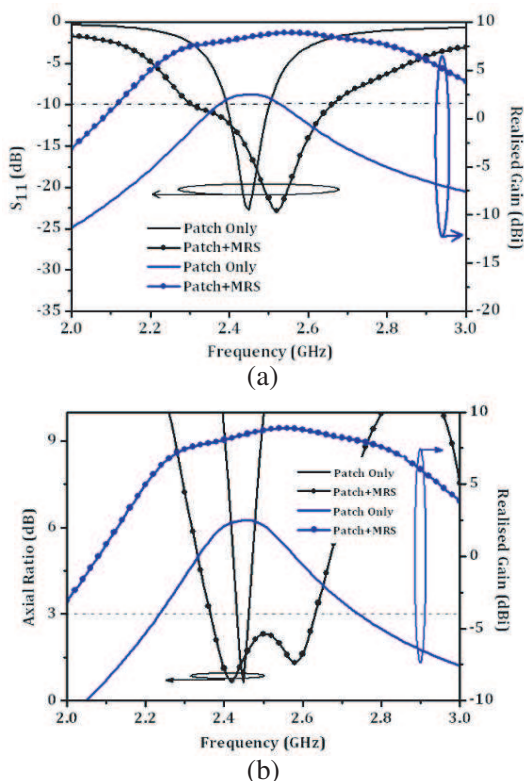


Figure 3. Comparison of simulated results for the CP-MPA with and without MRS. (a) Realized gain and S_{11} and (b) realized gain and ARBW with MRS at $h = 7.5$ mm.

(without the MRS cover), denoted as the reference antenna, is studied by simulation for comparison and discussion. The reference antenna has the same size as that of the CP source, $L = 30$ mm, while the truncated depth and the feed point are adjusted to $b = 4$ mm, $f_p = 10$ mm in order to have good impedance and axial-ratio matching for fair comparison.

The simulated results of the CP-MPA, along with those of MRS as well as the reference antenna are given in Fig. 3. We note that ZBW of the CP-MPA with MRS is 14.08% (2.31–2.66 GHz), whereas for the reference antenna it is only 4.08% (2.4–2.5 GHz), as shown in Fig. 3(a), demonstrating an enhancement of 350%. Fig. 3(b) shows both the realized gain and AR comparison between the two antennas. We can see that bandwidth for $AR \leq 3$ dB is increased from 1% to 11%

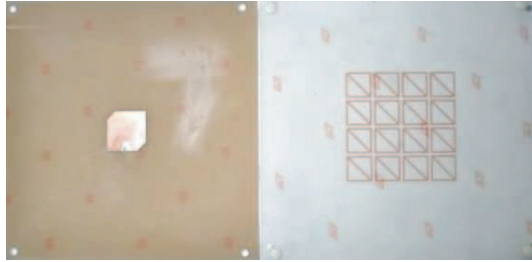


Figure 4. Photograph of a fabricated CP-MPA with MRS cover.

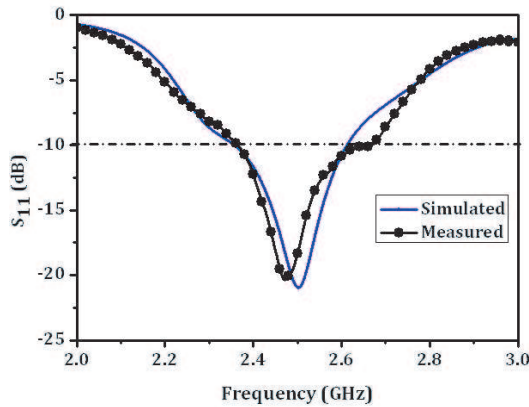


Figure 5. The simulated and measured S_{11} of the 4×4 SQR-DS as MRS with $h = 7.5$ mm.

by adding the MRS. The ARBW of the CP-MPA with MRS is 11% (296 MHz, 2.366–2.635 GHz), whereas for the reference antenna it is only 1.22% (30 MHz, 2.435–2.465 GHz), implying an improvement of 987%. Moreover, the realized gain of the CP-MPA with MRS is higher than that of the reference antenna. The maximum gains are 9.1 dBi and 2.4 dBi of CP-MPA with MRS and without MRS, respectively. This demonstrates that the proposed MRS has a remarkable effect on congregation of radiation energy in a low-profile format of an overall cavity height of 0.08λ .

The proposed CP-MPA with MRS was experimentally studied. The dimensions of the truncated patch antenna and the MRS were set, as described in Sec. 2.1. In order to verify the simulation results, an antenna prototype with 4×4 SQR-DS as MRS is fabricated; its photos are shown in Fig. 4. Fig. 5 shows the measured and simulated return losses of the CP-MPA with 4×4 SQR-DS. The measured ZBW

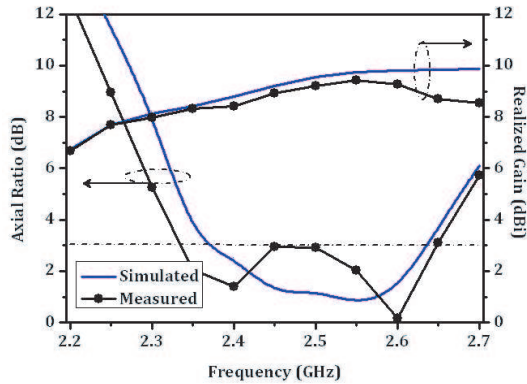


Figure 6. The measured and simulated gain and AR of the 4×4 SQR-DS as MRS with $h = 7.5$ mm.

is 11.93% (2.365–2.665 GHz) whereas the simulated one is 14.08% (2.31–2.66 GHz). The measured return-loss is in good agreement with the simulation, in general. The simulated and measured AR in the boresight direction ($\theta = 0^\circ$) of the antenna are shown in Fig. 6. Both the measured and simulated results show a good CP radiation performance. The measured 3-dB ARBW is 12.1% (2.33–2.64 GHz), which is wider than the simulated value of 10.0% (2.36–2.63 GHz) and it matches the measured ZBW. The minimum AR of 0.68 dB is recorded at 2.6 GHz.

The effects of the MRS covering the CP-MPA at a small height can be considered as two folds: (i) parasitic loading, and (ii) flat-plate cavity effect. The cavity effect is to put the MRS on top of a metallic ground plane so as to form a flat-plate cavity (FPC). The key part of the high-gain FPC antenna is its highly reflective surface. In the frequency range of 1.0–4.0 GHz as shown in Fig. 2(b), the highest reflectivity occurs at 3.5 GHz. At this frequency, one can make a FPC antenna, which would have the highest directivity. However, this requires a high profile of $\lambda_0/2$ and exhibits a narrow bandwidth. One of the simplest ways for broadening bandwidths is to reduce cavity's Q -factor at these frequencies, where MRS has a lower reflectivity; however, the cost is the reduction of gain and aperture efficiency. In other words, it is necessary to design the MRS with a stable reflectivity and also a phase response in a wide frequency range. In Fig. 2(b) and Fig. 2(c), the MRS has a magnitude difference of 0.2 and a phase difference of 20° , respectively, between 2.0 and 3.0 GHz. A trade-off between high gain and wide bandwidth can be realized by properly choosing the frequency range. Hence, this

frequency range is chosen because of its better frequency responses in terms of reflectivity and reflection phase. It is also called the non-resonant region [17], which is used for broadband and low-loss MTMs. In this frequency range, both permittivity ($\epsilon'_{eff} \gg 1$) and permeability ($0 < \mu'_{eff} < 1$) are nearly constant. From the effective medium point of view, the cavity consisting of the MRS behaves as a homogeneous material with a low effective refractive index (n). According to Snell's law of refraction, a low/near zero index material would make an electromagnetic wave emanates away from a primary source in any direction, to refract almost parallel to the normal of the surface of this material. This property provides a unique method of controlling the direction of emission and also the directivity enhancement. In summary, the MRS acts as a parasitic loading that increases the bandwidths (ZBW and ARBW) whereas the FP-cavity effect enhances the gain. These bandwidth enhancements are obtained mainly through the proximity coupling between the CP source patch and the MRS. This coupling mechanism is analogous to a two-layer electromagnetically-coupled patch (EMCP) antenna such that both the bandwidths can be improved [18]. The overlapped bandwidth is therefore determined by the AR bandwidth. Fig. 6 also shows the measured and simulated gain at the boresight of the antenna. The measured maximum gain of 9.4 dBi is recorded at 2.55 GHz whereas the simulated gain is 9.8 dBi at 2.69 GHz. The average measured gain is 8.5 dBi with a variation of less than 1 dB within the ARBW.

In order to understand the enhancement of ARBW by use of MRS, the distribution and phase of the simulated electric field at 2.45 GHz for the CP-MPA with MRS cover is illustrated in Fig. 7, where the direction of the arrow corresponds to the direction of the electric-field rotation. It is observed that a left-handed (clockwise) rotated current distribution is moving on the center of the patch. Gain enhancement of the antenna and the simulated electric field magnitude distribution for the CP-MPA with and without the MRS, are given in Fig. 8. It is important that the MRS made the field distribution of the aperture more uniform, and hence helped attain a higher gain. This means that the effective aperture is extended by adding the MRS.

Figure 9 shows the simulated and measured radiation patterns in the $\phi = 0^\circ$ and $\phi = 90^\circ$ planes for the CP-MPA with MRS at three frequencies-2.4, 2.5 and 2.6 GHz. For both planes, the left-hand (LH) circularly polarized fields are stronger than the right-hand (RH) circularly polarized fields, (more than 17 dB), in the boresight direction ($\theta = 0^\circ$). The front-to-back ratios of the left-hand polarization in both the $\phi = 0^\circ$ and $\phi = 90^\circ$ planes are more than 30 dB and 40 dB, respectively.

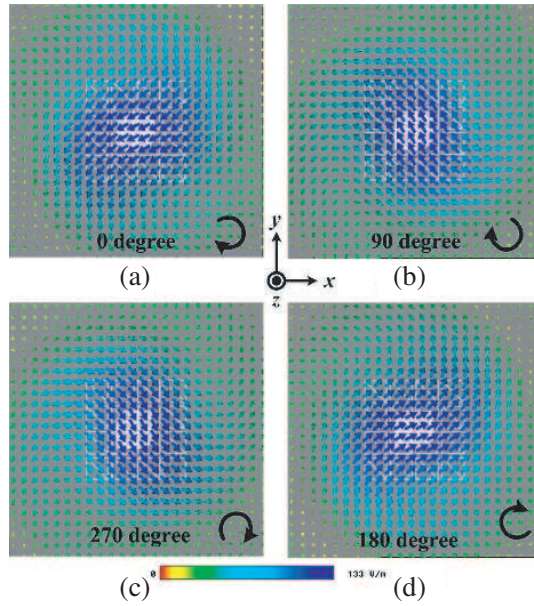


Figure 7. The distribution and phase of the simulated electric field at 2.45 GHz for the MRS covering the CP-MPA (a) 0 degree, (b) 90 degree, (c) 270 degree and (d) 180 degree.

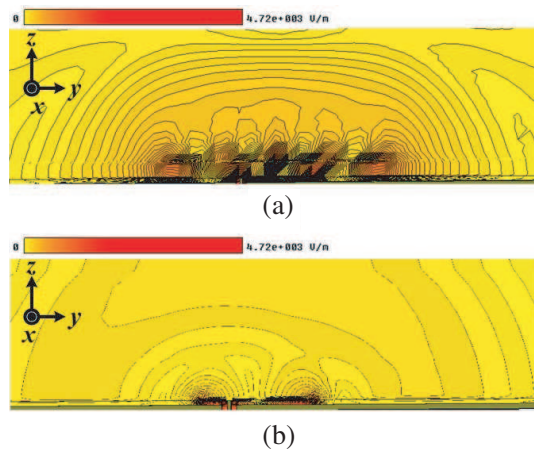


Figure 8. Electric field magnitude distribution at 2.45 GHz of the antennas (a) CP-MPA with MRS and (b) CP-MPA without MRS.

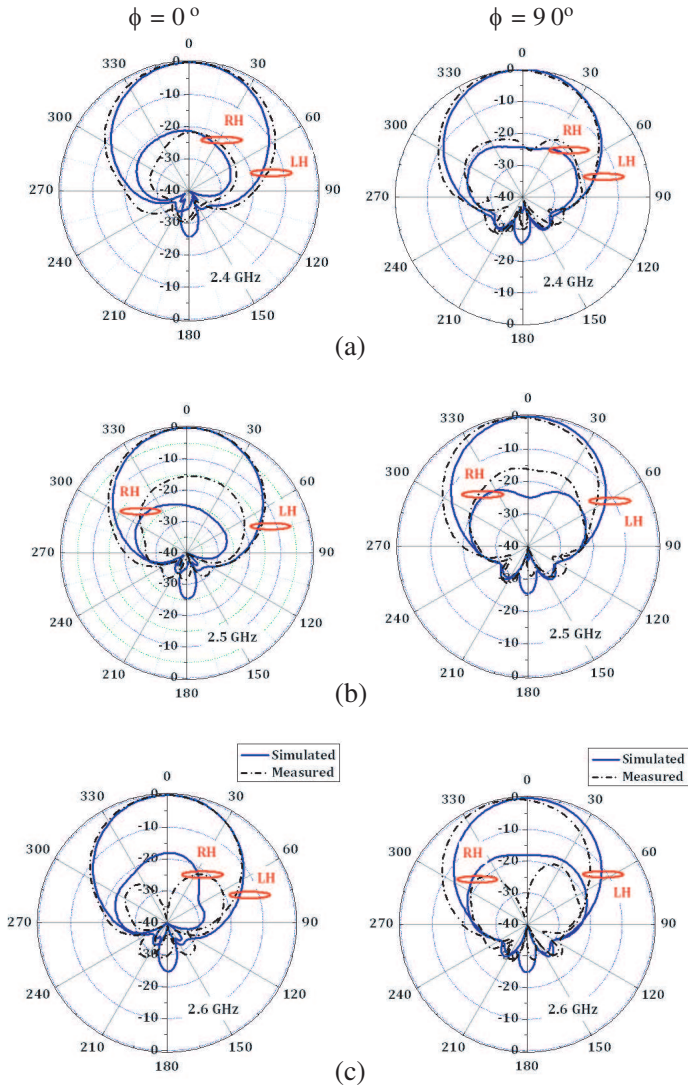


Figure 9. Measured and simulated radiation patterns in $\phi = 0^\circ$ and $\phi = 90^\circ$ planes of the 4×4 SQR-DS with a cavity height $h = 7.5$ mm (a) 2400 MHz, (b) 2500 MHz and (c) 2600 MHz.

4. CONCLUSION

This paper presents a new technique for simultaneous enhancement of gain, impedance bandwidth, axial-ratio bandwidth and gain bandwidth of a single-feed circularly polarized patch antenna. A planar metamaterial reflective surface (MRS) used as a superstrate and a directive-confining device for the 2.45 GHz conventional CP patch antenna, has been proposed, and its performances demonstrated. Simulation and experiment results confirm that impedance and axial ratio bandwidths, with realized gain, can be significantly improved by properly placing the MRS atop the CP source patch. The MRS is designed based on the μ -near-zero (MNZ) and high epsilon properties, which are considered as the source of gain enhancement. The proximity EM coupling of the MRS is regarded as the source for bandwidths enhancement. For the optimal results obtained in this study, the operating (overlapped) bandwidth can reach nearly 300 MHz with an average realized gain of 8.5 dBi for the proposed antenna in the 2.45 GHz ISM band. Currently, techniques used for further gain enhancement are being investigated; the results will be reported in a future publication.

ACKNOWLEDGMENT

The authors would like to acknowledge the Microwave and Wireless Communication Laboratory at the Chinese University of Hong Kong, for the assistance in the antenna measurement. This work was supported in part by the Hong Kong Polytechnic University, Grant No. ASA-16.

REFERENCES

1. Pozar, D. M. and D. H. Schaubert, *Microstrip Antennas*, IEEE Press, New York, 1995.
2. Guo, Y.-X., K.-W. Khoo, and L. C. Ong, "Wideband circularly polarized patch antenna using broadband baluns," *IEEE Trans. Antennas Propag.*, Vol. 56, No. 2, 319–326, Feb. 2008.
3. Kraff, U. R., "An experimental study on 2×2 sequential-rotation arrays with circularly polarized microstrip radiators," *IEEE Trans. Antennas Propag.*, Vol. 45, No. 10, 1459–1466, Oct. 1997.
4. Chung, K. L. and A. S. Mohan, "A circularly polarized stacked electromagnetically coupled patch antenna," *IEEE Trans. Antennas Propag.*, Vol. 52, No. 5, 1365–1370, May 2004.

5. Pirhadi, A., F. Keshmiri, M. Hakkak, and M. Tayarani, "Analysis and design of dual band high directive EBG resonator antenna using square loop FSS as superstrate layer," *Progress In Electromagnetics Research*, Vol. 70, 1–20, 2007.
6. Enoch, S., G. Tayeb, P. Sabouroux, N. Guerin, and P. Vincert, "A metamaterial for directive emission," *Phys. Rev. E*, Vol. 70, 016608, 2004.
7. Wu, B.-I., W. Wang, J. Pacheco, X. Chen, T. M. Grzegorzczuk, and J. A. Kong, "A study of using metamaterials as antenna substrate to enhance gain," *Progress In Electromagnetics Research*, Vol. 51, 295–328, 2005.
8. Silveririnha, M. and N. Engheta, "Design of matched zero-index metamaterials using nonmagnetic inclusions in epsilon-near-zero media," *Phys. Rev. B*, Vol. 75, 0751191–07511910, 2007.
9. Alu, A., N. Engheta, A. Erentok, and R. W. Ziolkowski, "Single-negative, double-negative, and low-index metamaterials and their electromagnetic applications," *IEEE Antennas and Propagat. Magazine*, Vol. 49, No. 1, Feb. 2007.
10. Gupta, K. C., "Narrow-beam antennas using an artificial dielectric medium with permittivity less than unity," *Electron Lett.*, Vol. 7, No. 1, 16–18, 1971.
11. Weng, Z.-B., Y.-C. Jiao, G. Zhao, and F.-Y. Zhang, "Design and experiment of one dimension and two dimension metamaterial structures for directive emission," *Progress In Electromagnetics Research*, Vol. 70, 199–209, 2007.
12. Chaimool, S., K. L. Chung, and P. Akkaraekthalin, "Bandwidth and gain enhancement of microstrip patch antenna using reflective metasurface," to be published in IEICE.
13. Lee, D. H., Y. J. Lee, J. Yeo, R. Mittra, and W. S. Park, "Directivity enhancement of circular polarized patch antenna using ring-shaped frequency selective surface superstrate," *Micro. Opt. Technol. Lett.*, Vol. 49, No. 1, 199–201, Jan. 2007.
14. Chang, T. N., M. C. Wu, and J.-M. Lin, "Gain Enhancement for circularly polarized microstrip patch antenna," *Progress In Electromagnetics Research B*, Vol. 17, 275–292, 2009.
15. Rahman, M. and M. A. Stuchly, "Circularly polarised patch antenna with periodic structure," *IEE Proc. - Microw. Antennas Propag.*, Vol. 149, No. 3, 141–146, June 2002.
16. Chen, H., B. I. Wu, L. Ran, T. M. Grzegorzczuk, and J. A. Kong, "Robust method to retrieve the constitutive effective parameters of metamaterials," *Phy Rev E*, Vol. 70, No. 1, 016608–0166015,

July 2004.

17. Liu, R., Q. Cheng, T. J. Cui, and D. R. Smith, *Broadband and Low-loss Non-resonant Metamaterials in Chapter 5, Metamaterials, Theory, Design and Applications*, Springer, New York Dordrecht Heidelberg London, 2010.
18. Chung, K. L. and A. S. Mohan, "A systematic design method to obtain broadband characteristics for singly-fed electromagnetically coupled patch antennas for circular polarization," *IEEE Trans. Antennas Propag.*, Vol. 51, No. 12, 3239–3248, Dec. 2003.